Surface Chemistry of Glycine on Pt{111} in different aqueous Environments

Andrey Shavorskiy[1,2], Tugce Eralp[1], Karina Schulte[3], Hendrik Bluhm[4], Georg Held[1] *

[1] University of Reading, Department of Chemistry, Whiteknights, Reading, RG6 6AD, UK

[2] Advanced Light Source, Lawrence Berkeley National Laboratory, Berkeley, CA 94720, USA

[3] MAX-lab, Lund University, 22100 Lund, Sweden

[4] Chemical Sciences Division, Lawrence Berkeley National Laboratory, Berkeley, CA 94720, USA

Revised version 31st May 2012

* **Corresponding address:**

University of Reading, Department of Chemistry

Whiteknights, Reading RG6 6AD UK

Email: g.held@reading.ac.uk

Abstract

Adsorption of glycine on Pt{111} under UHV conditions and in different aqueous environments was studied by XPS (UHV and ambient pressure) and NEXAFS. Under UHV conditions, glycine adsorbs in its neutral molecular state up to about 0.15 ML. Further deposition leads to the formation of an additional zwitterionic species, which is in direct contact with the substrate surface, followed by the growth of multilayers, which also consist of zwitterions. The neutral surface species is most stable and decomposes at 360 K through a multi-step process which includes the formation of methylamine and carbon monoxide. When glycine and water are co-adsorbed in UHV at low temperatures (< 170 K) inter-layer diffusion is inhibited and the surface composition depends on the adsorption sequence. Water adsorbed on top of a glycine layer does not lead to significant changes in its chemical state. When glycine is adsorbed on top of a pre-adsorbed chemisorbed water layer or thick ice layer, however, it is found in its zwitterionic state, even at low coverage. No difference is seen in the chemical state of glycine when the layers are exposed to ambient water vapor pressure up to 0.2 Torr at temperatures above 300 K. Also the decomposition temperature stays the same, 360 K, irrespective of the water vapor pressure. Only the reaction path of the decomposition products is affected by ambient water vapor.

1 Introduction

One of the great challenges in studying model surface systems related to bio-molecular heterogeneous catalysts lies in the fact that practically all relevant reactions take place in aqueous solutions near room temperature. Conventional surface science techniques cannot accurately study such adsorption/reaction complexes as the coadsorption of the relevant surface species cannot be modelled under reaction conditions in ultra-high vacuum (UHV). In UHV water only forms stable condensed layers below 150K [1, 2, 3], where the kinetic barriers are too high for many elementary steps of heterogeneous reactions, such as exchange of molecules between surface layer and solution and chemical reactions between the surface species. Reaction conditions for an aqueous solution/catalyst interface require temperatures where the vapour pressure is in the mbar/Torr range. This pressure range has recently become accessible for photoemission and X-ray absorption experiments, such as XPS and NEXAFS through new beam-line and detector designs [4, 5, 6].

Since amino acids are essential building blocks of living matter, their interaction with metal surfaces is an important area in the study of bio-inorganic interfaces with many applications in heterogeneous catalysis. To date, a number of studies of amino acid adsorption on copper surfaces (to some extent on gold and nickel surfaces) were conducted with an emphasis on enantiomeric effects in the adsorption of chiral amino acids [7, 8, 9, 10, 11, 12, 13, 14, 15, 16, 17, 18, 19, 20, 21, 22, 23, 24, 25, 26, 27, 28, 29, 30, 31, 32, 33]. Less attention was paid to the chemical composition of organic overlayers and their chemical interaction with metal surfaces, partly due to the low reactivity of the metals used in these studies at room temperature and partly because the application of copper-amino acid systems is very limited in heterogeneous catalysis. It has been shown in these studies that simple amino acids adsorb on Cu{110} in their anionic (de-protonated) form [10, 11, 15, 17, 22, 24, 28, 31] and are stable up to 450-500 K. Above this temperature complete desorption/decomposition occurs within a relatively small temperature window.

The exact decomposition mechanism depends on the specific amino acid. Our most recent work has shown that the decomposition process of alanine and glycine is dramatically affected by the presence of ambient water at pressures above 10^{-5} Torr, making the anion less stable [34].

Adsorption of small amino acids on Pt-group metal surfaces, which are commonly used as active components for heterogeneous catalysts, was studied experimentally with temperature-programmed desorption(TPD) and laboratory-based X-ray photoelectron spectroscopy (XPS) and theoretically using density functional theory (DFT) [35, 36, 37, 38, 39, 40, 41]. Particular attention was paid to the chemical composition at different temperatures. **The experimental studies report that adsorption of glycine and alanine on Pt{111} and Pd{111} leads to the formation of zwitterionic molecules, while DFT modeling favors neutral and anionic species [41]. Annealing of amino acid overlayers on these metals leads to the decomposition of molecules via C–C bond scission [35, 36, 37, 38].**

The current work aims at studying the influence of water on the surface chemistry of the smallest amino acid, glycine, with Pt{111}. Our particular emphasis is on comparing the dissociation behavior of glycine when the surface is exposed to water under UHV conditions and under ambient pressure conditions up to the Torr range. Surprisingly, the differences are very small, which is in stark contrast to earlier findings concerning the surface chemistry of glycine and alanine on Cu{110} [34].

2 Experiment

Most of the UHV experiments with Pt{111} were carried out at beamline I311 of the MAX-lab synchrotron facility in Lund, Sweden. The ambient pressure experiments were performed at beamline 11.0.2 of the Advanced Light Source (ALS) in Berkeley, USA. Both endstations consist of two ultrahigh-vacuum (UHV) chambers with base pressures in the

10^{-10} Torr range, which are described in detail elsewhere [42, 5, 43]. The preparation chambers are equipped with standard instruments for sample preparation and characterization (sputter gun, LEED). The analysis chamber at MAX-lab is equipped with a Scienta "SES 200" electron energy analyzer, which was used for the XPS and NEXAFS measurements; the sample temperature can be controlled between 100 K and 1200 K. The analysis chamber at ALS is dedicated to photoelectron spectroscopy at near-ambient-pressure conditions and is equipped with Specs Phoibos 150 electron spectrometer with custom-designed differentially pumped electron lenses [6, 44] which enable experiments up to water vapor pressures in the Torr range (0.2 Torr in the present case). At this endstation the sample temperature can be varied between 270 K and 1200 K.

Standard cleaning procedures were used for the Pt{111} surface, which include several cycles of sputtering and annealing to 1100 K in UHV and annealing cycles between 450 K and 750 K at an oxygen pressure of 1×10^{-7} mbar in order to remove residual carbon. Since it is known that surface impurities of the order of a few percent can have a dramatic effect on the behavior of water on metal surfaces [1, 2] we have ensured that the surface was clean to levels below the detection limits of XPS for oxygen and carbon (< 0.01 ML; 1 ML corresponds to 1 atom per substrate surface atom) before the start of each experiment. Glycine ($> 99\%$ pure, from Sigma-Aldrich) was dosed via sublimation at 140°C in vacuum from a home-build evaporation source, as described in [30, 45]. Even though the temperature of the evaporator was kept constant within 1°C the deposition rate was not constant over time, therefore the coverage was calibrated via the peak height of the N 1s XP signal. At MAX-lab water (HPLC-grade, further purified through 5 freeze-thaw cycles in vacuum) was dosed through a micro–capillary array doser at a distance of about 5 cm from the sample; at ALS, the sample was kept at a background pressure of water vapor.

During the XPS data acquisition the sample was slowly scanned with respect to the beam in order to avoid beam-induced damage to the adsorbate layers. The XP spectra

shown below were normalized with respect to the low binding energy (BE) background if not stated otherwise. For each spectrum the BE axis was calibrated by measuring the Fermi-edge (BE = 0) with the same beamline and analyzer settings as the actual spectrum. Temperature-programmed XP spectra (TP-XPS) were recoded as a series of fast XP spectra (typically 30 s per spectrum) while the sample was slowly annealed. Typical annealing rates were between 0.1 K/s (MAX-lab) and 0.3 K/s (ALS), which leads to a temperature resolution between 3 K and 9 K per spectrum.

NEXAFS spectra were acquired at MAX-lab in the Auger yield mode using the electron energy analyzer as detector. The O KLL Auger signal was detected in the kinetic energy range between 505 and 520 eV. The spectra were normalized with respect to the photon flux at the sample (I_0, measured trough a photodiode) and a background spectrum of the clean sample was subtracted.

3 Results

3.1 Adsorption on clean Pt{111}

Glycine adsorbs in its neutral molecular form on clean Pt{111} when the surface is held at 200 K. Figure 1 shows a series of C 1s, N 1s and O 1s XP spectra measured after glycine was deposited for the indicated times. The N 1s spectrum for the lowest coverage in the series, after 5 min dosing, in Figure 1(b) shows a single narrow peak with symmetric shape at BE 399.6 eV. This is characteristic for a neutral amino group ($H_2\mathbf{N}$) where the nitrogen atom forms a bond with the substrate, as it has been confirmed by several experimental and theoretical surface-crystallographic studies of amino acids adsorbed on Cu surfaces [11, 12, 18, 19, 24, 30, 34, 45, 33]. The O 1s spectrum of the same layer is shown in Figure 1(c). It shows a broad feature, which can be fitted by two peaks of similar intensity, indicating an intact carboxylic acid group with two non-equal types of oxygen atoms, C**O**OH and CO**OH**, at BE 531.4 eV and 533.3 eV, respectively. The

small difference in peak heights is probably due to photoelectron diffraction rather than a difference in the actual numbers of atoms. The corresponding C 1s spectrum in Figure 1(a) shows two well-resolved peaks, which can be assigned to carboxylic carbon (BE 288.8 eV) and the α-carbon atom (BE 285.8 eV) [11, 34]. The C 1s and N 1s spectra for low glycine coverage are in good agreement with earlier data from glycine/alanine adsorbed on Cu{110} [11, 24, 34]. All previous studies of glycine adsorption on metal surfaces, however, found a de-protonated carboxylate groups (identified by a single O 1s peak near BE 531.5 eV) for the molecules in direct contact with the metal, which enables surface bonds through both oxygen atoms [12, 45, 37, 38, 41]. This is obviously not the case here but the almost perfect overlap of the lower O 1s and the N 1s binding energies with those reported for Cu{110} [11, 24, 34] implies that the corresponding atoms, one oxygen and the nitrogen atom, are involved in the substrate bond on Pt{111}.

Upon further dosing at 200 K the neutral molecular species saturates and a new zwitterionic species of glycine is observed. After dosing for 10 min, new peaks appear in both the N 1s and C 1s regions of Figure 1(a,b), around BE 401 eV and 286.8 eV, respectively, which correspond to nitrogen and α-carbon atoms in the $\mathbf{N}H_3^{(+)}$-$\mathbf{C}H_2$-$COO^{(-)}$ zwitterion. The latter assignment is based on the fact that the binding energy is too low for carboxylate/carboxylic acid carbon atoms. The O 1s spectra of the same layer show an increase in the low-BE peak, which is now a superposition of contributions from the carboxylic acid -C**O**OH and carbolylate groups -C**OO**. Further dosing leads to an increase in the signals associated with the zwitterions and gradual attenuation of the signals originating from the neutral species. In addition, the high BE N 1s peak associated with $NH_3^{(+)}$ shifts continuously towards higher BE as the coverage increases. This indicates a gradual change in the adsorption geometry such that the N 1s core hole experiences less screening by the metal substrate. This could be caused by an increasing distance between the ammonium group and the substrate and/or by a reduced electron density at the metal surface due to charge transfer into the molecule. For the 70 min layer all peaks show shifts towards

higher BE, which is typical for multilayer formation with reduced screening by the metal. These latter spectra are very similar to those published by Löfgren et al. [36] for high coverages of glycine on Pt{111} (50×10^{14} molecules per cm^2, i.e. 3.3 ML); their low coverage spectra (4×10^{14} molecules per cm^2, i.e. 0.26 ML), however, also show a dominant signal around 402 eV in the N 1s region, which is in disagreement with our low coverage data.

The neutral species and the associated N 1s peak at BE 399.6 eV is the only one that saturates. Therefore we use the area of this peak as a measure of the glycine coverage and define a relative coverage of 1 (indicated as '1.0 Gly' in the Figures) such that it corresponds to a N 1s peak area equal to that of the saturated peak at BE 399.6 eV. The so-calculated relative coverages are indicated on the left-hand side of Figure 1(b). In the following we will concentrate on relative coverages between 1 and 2, where the neutral surface species dominates. By comparing the areas of the O 1s signal with that of a saturated chemisorbed water layer (0.7 ML), we find that 1.0 Gly corresponds to an absolute coverage of around 0.15 ML (i.e. 0.15 glycine molecules per surface Pt atom). Due to photoelectron diffraction effects, however, this calibration has a relatively large error bar. This low coverage, would to some extent explain the difference between the XP spectra in Ref. [36], where the low coverage spectra were recorded for 0.26 ML, and ours. It also implies that the saturated neutral glycine layer is not very densely packed and that there is room for additional zwitterionic molecules in direct contact with the substrate surface. Ernst and Christman observed a $p(2 \times 2)$ LEED pattern, which is associated with a coverage of 0.25 ML [35]. Even a coverage of 0.33 ML would be possible for flat-lying molecules from a purely steric point of view. We must, therefore, assume that at higher coverages not all molecules in direct contact with the metal surface are neutral.

Several other experimental findings also suggest that some of the zwitterionic molecules form strong bonds with the substrate. First, when a multilayer coverage is annealed to 330 K, i.e. above the multilayer desorption temperature [36], not all of the XP signal

associated with the zwitterionic species disappears. An example is shown in the middle spectra of Figure 1 (40 min dose annealed to 330 K), which shows a ratio of around 1.5 : 1 between NH_3 and NH_2 N 1s signals (rel. coverage 2.5). This indicates that the surface bond of the zwitterions in this layer is stronger than that of the multilayer.

Second, the Pt $4f_{7/2}$ spectra show that the surface core level shifts are also affected by the zwitterionic species. Figure 2 shows photoelectron spectra of the Pt $4f_{7/2}$ line for several glycine coverages together with a spectrum of the clean surface for comparison. In order to account for the attenuation through the adsorbate layer, all spectra are normalized with respect the total area under the curve. The spectrum of the clean surface contains two well-resolved peaks marked 'B' for bulk and 'S' for surface platinum atoms. The surface core-level shift of the S state with respect to B, -0.42 eV, is in excellent agreement with previously reported experimental data, which range between -0.37 eV and -0.42 eV [46, 47]. Adsorption of glycine first leads to a decrease of the surface signal (5 min / 0.7 Gly layer) followed by the appearance of a shoulder at the high BE side of the spectrum, which is associated with a new peak at 71.3 eV. The appearence of this latter peak seems to be correlated with the zwitterionic signal in the N 1s spectra rather than the neutral species and saturates between the spectra for the 10 min (rel. coverage 1.4) and 15 min (rel. coverage 2.5) layers. The relative area under the clean surface 'S' peak decreases up to the 10 min spectrum and stays more or less constant at around $\frac{1}{3}$ of the clean surface value thereafter, implying that not all surface Pt atoms are involved in a bond with the adsorbate. Although the relative peak areas of substrate surface peaks are often strongly affected by photoelectron diffraction, the observed trend suggests that the glycine layer in direct contact with the substrate reaches saturation between 1.4 Gly and 2.5 Gly at 200 K. By comparison with the data in Figure 1 we therefore conclude that this layer consists of neutral (carboxylic acid) and zwitterionic species.

Third, the O NEXAFS spectra in Figure 3 show strong polar anisotropy of the π^*-resonance at 532 eV for both the pure neutral species ('1.1 Gly') and a layer with an

approximate 2 : 1 ratio of zwitterionic and neutral species ('3.2 Gly'). This resonance is associated with an unoccupied π-orbital on the carboxylate group. The selection rules are such that the cross section is close to zero if the polarization vector, $\vec{E}$, is parallel to the plane of the O-C-O triangle. The fact that the π^*-resonance intensity almost disappears for normal incidence ($\vec{E}$ 90° with respect to the surface normal) therefore indicates that the carboxylate groups are almost parallel to the Pt surface. For thicker multilayers of glycine ('multil. Gly') the NEXAFS spectra do not show any anisotropy in the π^*-resonance.

As mentioned above, when a multilayer coverage of glycine is annealed to 330 K, all but the chemisorbed layer desorb as intact molecules [36]. In the chemisorbed layer above 330 K neutral and zwitterionic species of glycine co-exist at a ratio of 1 : 1.5 (cf Figure 1, middle spectra, rel. coverage 2.5). A sequence of annealing steps between 250 K and 505 K of a lower coverage glycine layer is shown in Figure 4. The layer remains unchanged upon annealing up to 325 K. Annealing to 350 K leads to the desorption of zwitterionic glycine (N 1s BE 401 eV) competing with decomposition, whereas the neutral molecular species (N 1s BE 399.6 eV) is stable up to 350 K (Figure 4 (a,b,c)). The O 1s spectrum in Figure 4(c) shows a weak additional feature at BE 530.9 eV after annealing to 350 K, which is associated with the formation of CO. The corresponding C 1s peak overlaps with the α-carbon signal at 285.8 eV. Above 350 K all glycine molecules undergo rapid decomposition, which is characterized by the disappearance of the N 1s peaks corresponding to amino-nitrogen and the C 1s peaks corresponding to carboxylic and α- carbon. A number of decomposition products are formed on the surface during the decomposition process of which CO (C 1s BE 286.1/286.9 eV; O 1s BE 530.9/532.7 eV) and $H_xC{=}N$ with $x = 1, 2$ (C 1s BE 284.0/284.8 eV, N 1s BE 396.7/398.6 eV) are the most likely species [35, 36]. CO desorbs between 400 K and 425 K while the $H_xC{=}N$ surface species undergo several modifications and are stable up to about 500 K. The exact chemical composition, in the temperature range above 350 K depends strongly on the initial coverage, heating rate and the quality (roughness) of the substrate.

3.2 Co-adsorption with water in UHV

Under UHV conditions water desorbs from clean Pt{111} at around 160 K [2, 3]. Co-adsorption with atomic adsorbates, such as oxygen, and the formation of stable hydrogen-bonded networks can delay desorption up to 200 K [48, 49, 50], however the co-adsorption with glycine does not appear to have a significant stabilizing effect. At temperatures below 200 K the surface chemistry is mostly determined by kinetic effects rather than equilibrium thermodynamics. In particular, inter-layer diffusion is strongly hindered, hence, the composition of the surface layer strongly depends on the adsorption sequence. Deposition of a water layer onto pre-adsorbed glycine layers at 145 K ('H_2O / Gly / Pt{111}') does not lead to significant changes in adsorption properties of the amino acid. The bottom part of Figure 5(a,b,c) shows C 1s, N 1s and O 1s spectra obtained after dosing 0.7 ML water onto a glycine layer of relative coverage 1.2 at 145 K. Also shown are spectra of the same layer before water was adsorbed. The C 1s and N 1s spectra show no significant changes in peak positions and shape. Only small BE shifts are observed due to the formation of hydrogen bonds and/or extra screening by the surrounding water molecules. The angular dependence of the oxygen NEXAFS spectra for this layer (dashed lines in Figure 3) is less pronounced than for the pure glycine layer, which indicates some orientational change towards a more tilted geometry of the carboxylic acid group.

The situation is different when glycine is deposited onto a Pt{111} surface pre-covered with a thin water layer ('Gly / H_2O / Pt{111}'). The top parts of Figure 5(a,b,c) show spectra of a similar coverage of glycine (rel. coverage 1.4) adsorbed at 145 K onto a bilayer of chemisorbed water (0.7 ML) on Pt{111}. The spectral features in the C 1s and N 1s regions at 145 K are clearly similar to those of zwitterionic glycine in the multilayer and not the chemisorbed neutral species. The angular dependence of the corresponding oxygen NEXAFS spectra (Figure 3) is very similar to the H_2O / Gly layer (dashed lines), whereas adsorption of the same amount of glycine onto thicker layers of water, 'Gly/ ASW'

(amorphous solid water, bottom spectra in Figure 3) leads to the loss of anisotropy in the O NEXAFS spectra. Both the NEXAFS and XPS features related to glycine in this layer are identical to those of multilayer glycine. Annealing to 265 K leads to the desorption of water leaving behind a glycine layer which is spectroscopically indistinguishable from the layers of similar coverage prepared by deposition at 200 K (Figure 1). Figure 5(c) shows a TP-XPS plot of the N 1s region of glycine (rel. coverage 1.2) on 0.7 ML water during annealing from 160 K to 250 K. Water desorption occurs at around 170 K, as can be seen from the change in the background intensity near the N 1s signal (not visible in Fig. 5 where the background is subtracted from the spectra). The conversion form the zitterionic into the neutral molecular species occurs at a slow rate between 170 K and 220 K after the complete desorption of the water layer.

3.3 Exposure to water under ambient pressure conditions

In the ambient pressure experiments stable water layers could not be maintained on Pt{111} at room temperature even at the highest water vapor pressure, 0.2 Torr. The experiments were carried out by pre-adsorbing glycine layers of relative coverages around 1.5 at 300 K in UHV and exposing these layers to various ambient pressures of water between 1×10^{-5} Torr and 0.2 Torr. After each exposure to elevated water pressures survey spectra were recorded, which did not show any contamination in addition to the signals mentioned below.

Figure 6 shows a comparison of C 1s, N 1s and O 1s spectra recorded under UHV conditions and at the maximum ambient pressure or 0.2 Torr. The C 1s and N 1s spectra show additional features at BE 285.9 eV and 396.9 eV, respectively, compared to those recorded after adsorbing glycine at 200 K, which are due to decomposition that occurs during adsorption at this higher temperature. The main outcome of these experiments is, however, that there is no change in those spectra when the layer is exposed to water. The only difference is seen in the O 1s spectra, where an extra peak is observed at 535.2 eV

due to photoelectron emission from gas-phase water molecules. No significant signal due to water adsorption (BE 532-534 eV) can be detected nor are there any signs of new surface species in the C 1s and N 1s spectra.

When we compare the temperature dependence of layers exposed to different ambient pressures of water we also find little difference in the dissociation kinetics up to about 380 K. Figure 7(a,b) show N 1s TP-XPS plots between 300 K and 550/470 K of glycine layers of relative coverage 1.5 in UHV (a) and 0.2 Torr water (b). In both cases the decomposition of glycine occurs at 360 K, as indicated by a sudden change of the N 1s signal. The diagram in Figure 7(c) shows the area of the NH_2 peak of glycine (BE 399.6 eV) as a function of temperature for all ambient pressures studied in this work. The disappearance of this peak marks the decomposition of glycine which occurs at the same temperature, 360 ± 5 K (at the 50% point), for all pressures. Note that the scatter of decomposition temperatures is determined by the temperature resolution of the TX-XPS experiments (ca. 10 K per spectrum).

After decomposition two new features appear at BE 396.7 eV and 398.6 eV, both of which were assigned to H_xCN species (see discussion of Figure 4(b)). In ambient water pressure above 10^{-3} Torr these species are stable up to 420 K and react with water to form a volatile product that desorbs from the surface immediately. Below 10^{-3} Torr the same H_xCN species decompose on the surface at 380 K leaving behind, what is most likely a CN species with a N 1s BE of 397.2 eV. Note, in the TPXPS series this transition occurs at a lower temperature than in the stepwise annealing UHV experiments, cf. Figure 4, because the sample is kept at high temperatures during the entire experiment. The stability of this latter species is affected even by relatively low ambient water pressures. At 10^{-5} Torr the signal disappears at 430 K whereas in UHV it is observed up to 500 K.

In summary, the main effect of ambient water vapor is stabilizing the H_xCN decomposition products above 380 K and providing additional pathways for their surface reactions. There is, however, no evidence for a substrate-catalyzed surface reaction between water

and glycine itself on Pt{111}.

4 Discussion

Our experiments clearly show that glycine adsorbs on Pt{111} in its neutral molecular state (H_2NCH_2COOH) at low coverage, both in UHV and under ambient water vapor pressure up to 0.2 Torr (the highest pressure for which XPS measurements were conducted). This is in contrast to the adsorption states that were observed experimentally for glycine and other small amino acids adsorbed on other late transition metals, such as Cu [11, 10, 12, 22, 17, 24, 51, 28, 15, 52, 30, 31, 32] and Pd [37, 38, 39], for which either anionic ($H_2NCH_2COO^{(-)}$) or zwitterionic ($H_3N^{(+)}CH_2COO^{(-)}$) species are reported, even at the smallest coverage. Also earlier experimental studies of glycine on Pt{111} [35, 36] report that the molecule is in its zwitterionic state but this disagreement is likely to be due to higher coverages (rel. coverage > 1) in these studies, where we also observe zwitterionic glycine. Our results are in agreement with recent DFT model calculations by Han et al. [41], which predict that the neutral state would be most stable for glycine on Pt{111} whereas the de-protonated anionic state is most stable for Cu and Pd surfaces, although the dissociation barrier is very high in the latter case.

The neutral molecular species is stable up to 360 K and saturates at 0.15 ML. Further adsorption of glycine is in the zwitterionic state. Some of the zwitterionic species adsorbs either in direct contact with the substrate or is very strongly bound to the chemisorbed neutral species at a ratio of around 1 : 1.5 (neutral to zwitterionic). Again, the model calculations by Han et al. [41] indicate that stabilization through hydrogen bonds can favor zwitterions over neutral glycine when clusters are formed in two or three dimensions.

In its crystalline form [53] and in aqueous solution under neutral conditions glycine is most stable as zwitterion compared to other forms, namely molecular, anionic or cationic. The interaction between glycine and liquid water or ice has been studied theoretically and

experimentally in recent years [54, 55, 56, 57, 58, 59, 60, 61]. In aqueous solutions at neutral pH zwitterions form hydrogen bonds with up to 8 water molecules [54, 62, 56, 61]. In solutions with high concentrations of protons (pH < 2.35) or hydroxyl (pH > 9.78) glycine is cationic or anionic, respectively. The interaction of glycine with ice or solid amorphous water is usually hydrophobic [55, 60]. For example, in mixed glycine-ice films on alumina a phase separation into solid glycine and water ice was observed in UHV at 110 K - 150 K whereby glycine segregates at the ice surface, predominantly in its zwitterionic state but with some anionic contribution ($H_2NCH_2COO^{(-)}$) [60]. Co-adsorption of glycine and water ice on TiO_2 in UHV at 160 K leads to similar hydrophobic behavior of glycine [55]. As TiO_2 binds stronger to glycine than to H_2O, however, the latter is completely displaced from the surface. On Calcite{104} glycine adsorbs from aqueous solution on top of a wetting water layer [57]. In all the above examples glycine was found or assumed to be in its zwitterionic state. One might therefore expect that glycine would also change its state on Pt{111} to zwitterionic when it is co-adsorbed with water. But our results clearly show that glycine remains in it neutral state, even in ambient water pressure and temperatures around 300 K, where the associated kinetic barriers should not prevent it from assuming its equilibrium state. The only exception is when glycine is adsorbed onto a pre-adsorbed water-ice layer at low temperature. In this case interlayer diffusion is kinetically hindered and glycine stays on the ice layer in its zwitterionic state.

The neutral state of glycine is the energetically preferred surface species on Pt{111} at low coverage. According to the DFT calculations by Han et al. [41] for pure glycine the energy difference is 0.24 eV and 0.52 eV with respect to the anionic and zwitterionic state, respectively. The substrate bond is through the amino group and one oxygen atom, which allows two strong hydrogen bonds between the molecules. The energy contribution from additional hydrogen bonds with water, which would be possible in the zwitterionic state, do not seem to be not sufficient to overcome this difference. Therefore glycine remains in the neutral state when in contact with water.

A related system that we have studied in a similar way, glycine on Cu{110}, behaves very differently [34]. There, the preferred adsorption species is the de-protonated anionic form of glycine, which is stable in UHV up to 480 K. Ambient water at pressures above 10^{-5} Torr reduces the stability of the surface species and induces dissociation at significantly lower temperatures, as low as 400 K at 10^{-1} Torr. The loss of stability was explained by the availability of additional dissociation channels when water and/or it's decomposition products are present at the surface.

At first, it must be noted that the overall thermal stability of glycine is lower on Pt{111} compared to Cu{110}. Dissociation takes already place at 360 K, independent of the magnitude of ambient water pressure. An effect of ambient water is only seen in the thermal development after dissociation. The decomposition of glycine on Pt{111} is a multi-step process involving the formation of a number of intermediate products. The exact composition in a multicomponent surface layer cannot always be determined unambiguously by XPS, as different species can have overlapping peaks and/or different adsorption sites of the same species (e.g. CO) will lead to multiple signals [63]. It is therefore important to check the interpretation of XPS results with other methods. Löfgren et al. [36] and Ernst & Christmann [35] have studied the decomposition pathway of glycine on Pt{111} by means of TPD to reveal the formation of methylamine via C-C bond scission as a first step followed by immediate further decomposition into smaller surface species and volatile molecules, as methylamine is not stable on Pt{111} [64, 65]:

$$(H_2N)CH_2COOH \rightarrow (H_2N)CH_2 + COOH \rightarrow H_xCN^{ads},\ CO^{ads},\ {CO_2}^{gas},\ {H_2}^{gas}\ {H_2O}^{gas}$$

These findings are compatible with our interpretation of the XP spectra at higher temperatures. Similar decomposition pathways were also observed for simple amino acids on Pd{111} and Cu{110} [37, 38, 39, 66, 22, 34]. The effect of ambient water is to stabilize the intermediate methylamine species and to facilitate their direct conversion into volatile species. Similar to the case of glycine on Cu{110}, the most likely mechanisms are either surface-catalyzed hydrogenation or oxidation through decomposition products of water

(H, O, OH) that are present on the Pt{111} surface under ambient conditions.

5 Summary and Conclusions

Under UHV conditions, glycine adsorbs in its neutral form up to about 0.15 ML (rel. coverage 1.0). This state has not been reported in earlier spectroscopic studies of this adsorption system [36]. Additional molecules adsorb as zwitterions. Up to a relative coverage of 2.5 these are strongly bound to the substrate surface, either directly or via the neutral molecules. Multilayer growth is observed for higher coverages. These multilayers desorb intact below 330 K, the more strongly bound zwitterions desorb between 330 K and 350 K and the neutral species decomposes at 360 K in a multi-step process that includes the formation of methylamine and carbonmonoxide.

Co-adsorption with water under UHV conditions requires low temperatures (< 170 K) and leads to surface compositions that strongly depend on the adsorption sequence due to a lack of inter-layer diffusion. When glycine is adsorbed first and water second (H_2O / Gly) the chemical state of glycine is the same as without water. When water is adsorbed first, either a chemisorbed layer or a thicker layer of amorphous solid water, glycine is found in its zwitterionic state, similar to multilayers.

Co-adsorption of glycine and water under ambient water pressures up to 0.2 Torr and temperatures above 300 K has no effect on the chemical state of low coverages of glycine, nor on the decomposition temperature. The main effect of ambient water vapor is stabilizing the H_xCN decomposition products above 380 K and providing additional pathways for their surface reactions. There is no evidence for a substrate-catalyzed surface reaction between water and intact glycine on Pt{111}. In this particular case, the results obtained from UHV experiments regarding the chemical state of glycine in the temperature range below 360 K are also valid in ambient water pressures. This is, however, not generally true.

Acknowledgement

This work was supported by the European Community through the Marie Curie Early Stage Training Network "MONET" (MEST-CT-2005-020908) and by the European Community Research Infrastructure Action under the FP6 "Structuring the European Research Area" program (through the Integrated Infrastructure Initiative "Integrating Activity on Synchrotron and Free Electron Laser Science"). The Advanced Light Source is supported by the Director, Office of Science, Office of Basic Energy Sciences, of the U.S. Department of Energy under Contract No. DE-AC02-05CH11231. The authors would like to thank the staff of both MAX-lab and ALS for their support.

References

[1] P. A. Thiel and T. E. Madey, Surf. Sci. Rep. **7** (1987) 221.

[2] M. A. Henderson, Surf. Sci. Rep. **46** (2002) 1.

[3] A. Hodgson and S. Haq, Surf. Sci. Rep. **64** (2009) 381.

[4] D. F. Ogletree, H. Bluhm, G. Lebedev, C. S. Fadley, Z. Hussain and M. Salmeron, Rev. Sci. Instr. **73** (2002) 3872.

[5] H. Bluhm, K. Andersson, T. Araki, K. Benzerara, G. Brown, J. Dynes, S. Ghosal, M. Gilles, H.-C. Hansen, J. Hemminger, A. Hitchcock, G. Ketteler, A. Kilcoyne, E. Kneedler, J. Lawrence, G. Leppard, J. Majzlam, B. Mun, S. Myneni, A. Nilsson, H. Ogasawara, D. Ogletree, K. Pecher, M. Salmeron, D. Shuh, B. Tonner, T. Tyliszczak, T. Warwick and T. Yoon, J. El. Spec. Rel. Phenomena **150** (2006) 86.

[6] H. Bluhm, J. El. Spec. Rel. Phenomena **177** (2010) 71.

[7] S. M. Barlow and R. Raval, Surf. Sci. Rep. **50** (2003) 201.

[8] G. Held and M. J. Gladys, Top. Catal. **48** (2008) 128.

[9] J. Williams, S. Haq and R. Raval, Surf. Sci. **368** (1996) 303.

[10] S. M. Barlow, K. J. Kitching, S. Haq and N. V. Richardson, Surf. Sci. **401** (1998) 322.

[11] J. Hasselström, O. Karis, M. Weinelt, N. Wassdahl, A. Nilsson, M. Nyberg, L. G. M. Petterson, M. G. Samant and J. Stöhr, Surf. Sci. **407** (1998) 221.

[12] N. A. Booth, D. P. Woodruff, O. Schaff, T. Gießel, R. Lindsay, P. Baumgärtel and A. M. Bradshaw, Surf. Sci. **397** (1998) 258.

[13] X. Zhao, Z. Gai, R. G. Zhao, W. S. Yang and T. Sakura, Surf. Sci. **424** (1999) L347.

[14] X. Zhao, R. G. Zhao and W. S. Yang, Langmuir **16** (2000) 9812.

[15] M. Nyberg, J. Hasselström, O. Karis, N. Wassdahl, M. Weinelt, A. Nilsson and L. G. M. Petterson, J. Chem. Phys. **112** (2000) 5420.

[16] Q. Chen, D. J. Frankel and N. V. Richardson, Surf. Sci. **497** (2002) 37.

[17] V. Efstathiou and D. Woodruff, Surf. Sci. **531** (2003) 304.

[18] R. B. Rankin and D. S. Sholl, Surf. Sci. **548** (2004) 301.

[19] R. B. Rankin and D. S. Sholl, Surf. Sci. Lett. **574** (2005) L1.

[20] R. B. Rankin and D. S. Sholl, J. Phys. Chem. B **109** (2005) 16764.

[21] D. I. Sayago, M. Polcik, G. Nisbet, C. L. A. Lamont and D. P. Woodruff, Surf. Sci. **590** (2005) 76.

[22] S. M. Barlow, S. Louafi, D. Le Roux, J. Williams, C. Muryn, S. Haq and R. Raval, Surf. Sci. **590** (2005) 243.

[23] X. Zhao and J. Rodriguez, Surf. Sci. **600** (2006) 2113.

[24] G. Jones, L. B. Jones, F. Thibault–Starzyk, E. A. Seddon, R. Raval, S. J. Jenkins and G. Held, Surf. Sci. **600** (2006) 1924.

[25] S. Blankenburg and W. G. Schmidt, Nanotechnology **18** (2007) 424030.

[26] M. J. Gladys, A. V. Stevens, N. R. Scott, G. Jones, D. Batchelor and G. Held, J. Phys. Chem. C **111** (2007) 8331.

[27] S. Haq, A. Massey, N. Moslemzadeh, A. Robin, S. M. Barlow and R. Raval, Langmuir **23** (2007) 10694.

[28] V. Humblot, C. Methivier, R. Raval and C.-M. Pradier, Surf. Sci. **601** (2007) 4189.

[29] L. Thomsen, M. Wharmby, D. P. Riley, G. Held and M. J. Gladys, Surf. Sci. **603** (2009) 1253 .

[30] T. Eralp, Z. V. Zheleva, A. Shavorskiy, V. R. Dhanak and G. Held, Langmuir **26** (2010) 10918.

[31] T. Eralp, A. Shavorskiy, Z. V. Zheleva, G. Held, N. Kalashnyk, Y. Ning and T. R. Linderoth, Langmuir **26** (2010) 18841.

[32] T. Eralp, A. Shavorskiy and G. Held, Surf. Sci. **605** (2011) 468.

[33] T. Eralp, A. Ievins, A. Shavorskiy and G. Held, J. Am. Chem. Soc. in press, DOI:10.1021/ja210499m.

[34] A. Shavorskiy, F. Aksoy, M. E. Grass, Z. Liu, H. Bluhm and G. Held, J. Am. Chem. Soc. **133** (2011) 6659.

[35] K. H. Ernst and K. Christmann, Surf. Sci. **224** (1989) 277.

[36] P. Löfgren, A. Krozer, J. Lausmaa and B. Kasemo, Surf. Sci. **370** (1997) 277.

[37] F. Gao, Z. Li, Y. Wanga, L. Burkholder and W. T. Tysoe, J. Phys. Chem. C **111** (2007) 9981 .

[38] F. Gao, Z. Li, Y. Wang, L. Burkholder and W. T. Tysoe, Surf. Sci. **601** (2007) 3276.

[39] F. Gao, Y. Wang, L. Burkholder and W. T. Tysoe, Surf. Sci **601** (2007) 3579.

[40] J. N. James and D. A. Sholl, Curr. Opinion Colloid Interface Science **13** (2008) 60.

[41] J. W. Han, J. N. James and D. S. Sholl, J. Chem. Phys. **135** (2011) 034703.

[42] R. Nyholm, J. N. Andersen, U. Johansson, B. N. Jensen and I. Lindau, Nucl. Instr. Methods Phys. Res. Sect A **467** (2001) 520.

[43] D. F. Ogletree, H. Bluhm, E. L. D. Hebenstreit and M. Salmeron, Nuclear Instruments and Methods in Physics Research A **601** (2009) 151.

[44] M. E. Grass, P. G. Karlsson, F. Aksoy, M. Lundqvist, B. Wannberg, B. S. Mun, Z. Hussain and Z. Liu, Rev. Sci. Instrum. **81** (2010) 53106.

[45] Z. V. Zheleva, T. Eralp, and G. Held, J. Phys. Chem. C **116** (2012) 618.

[46] R. Denecke and N. Mårtensson, *Adsorbate induced surface core level shifts of metals*, Vol. III/42A4 of *Landolt-Börnstein Numerical Data and Functional Relationships in Science and Technology, Newseries*, Springer, Berlin (2005) pg. 388.

[47] L. Bianchettin, A. Baraldi, S. de Gironcoli, E. Vesselli, S. Lizzit, L. Petaccia, G. Comelli and R. Rosei, J. Chem. Phys. **128** (2008) 114706.

[48] C. Clay, S. Haq and A. Hodgson, Phys. Rev. Lett. **92** (2004) 46102.

[49] T. Schiros, L.-A. Näslund, K. Andersson, J. Gyllenpalm, G. S. Karlberg, M. Odelius, H. Ogasawara, L. G. M. Pettersson and A. Nilsson, J. Phys. Chem. C **111** (2007) 15003.

[50] A. Shavorskiy, M. Gladys and G. Held, Phys. Chem. Chem. Phys. **10** (2008) 6150.

[51] G. Gonella, S. Terreni, D. Cvetko, A. Cossaro, L. Mattera, O. Cavalleri, R. Rolandi, A. Morgante, L. Floreano and M. Canepa, J. Phys. Chem. B **109** (2005) 18003.

[52] Y. Zubavichus, M. Zharnikov, A. Schaporenko and M. Grunze, J. El. Spec. Rel. Phen. **134** (2004) 25.

[53] R. E. Marsh, Acta Cryst. **11** (1958) 654.

[54] M. J. Campo, J. Chem. Phys. **125** (2006) 114511.

[55] J. Lausmaa, P. Löfgren and B. Kasemo, J. Bio. Mat. Res. A **44** (1999) 227.

[56] K. Leung and S. B. Rempe, J. Chem. Phys. **122** (2005) 184506.

[57] U. Magdans, X. Torrelles, K. Angermund, H. Gies and J. Rius, Langmuir **23** (2007) 4999.

[58] M. Parsons and Y. Koga, J. Chem. Phys. **123** (2005) 234504.

[59] P. Schravendijk, L. Ghiringhelli, L. Site and N. van der Vegt, J. Phys. Chem. C **111** (2007) 2631.

[60] M. Tzvetkov, M. G. Ramsey and F. P. Netzer, J. Chem. Phys. **122** (2005) 114712.

[61] S. Xu, J. M. Nilles and K. H. Bowen, J. Chem. Phys. **119** (2003) 10696.

[62] K. Chuchev and J. J. BelBruno, J. Mol. Struct: THEOCHEM **850** (2008) 111.

[63] G. Held, J. Schuler, W. Sklarek and H.-P. Steinrück, Surf. Sci. **398** (1998) 154.

[64] S. Hwang, E. Seebauer and L. Schmidt, Surf. Sci. **188** (1987) 219.

[65] D.-H. Kang and M. Trenary, Surf. Sci. **519** (2002) 40.

[66] J. J. Chen and N. Winograd, Surf. Sci. **326** (1995) 285.

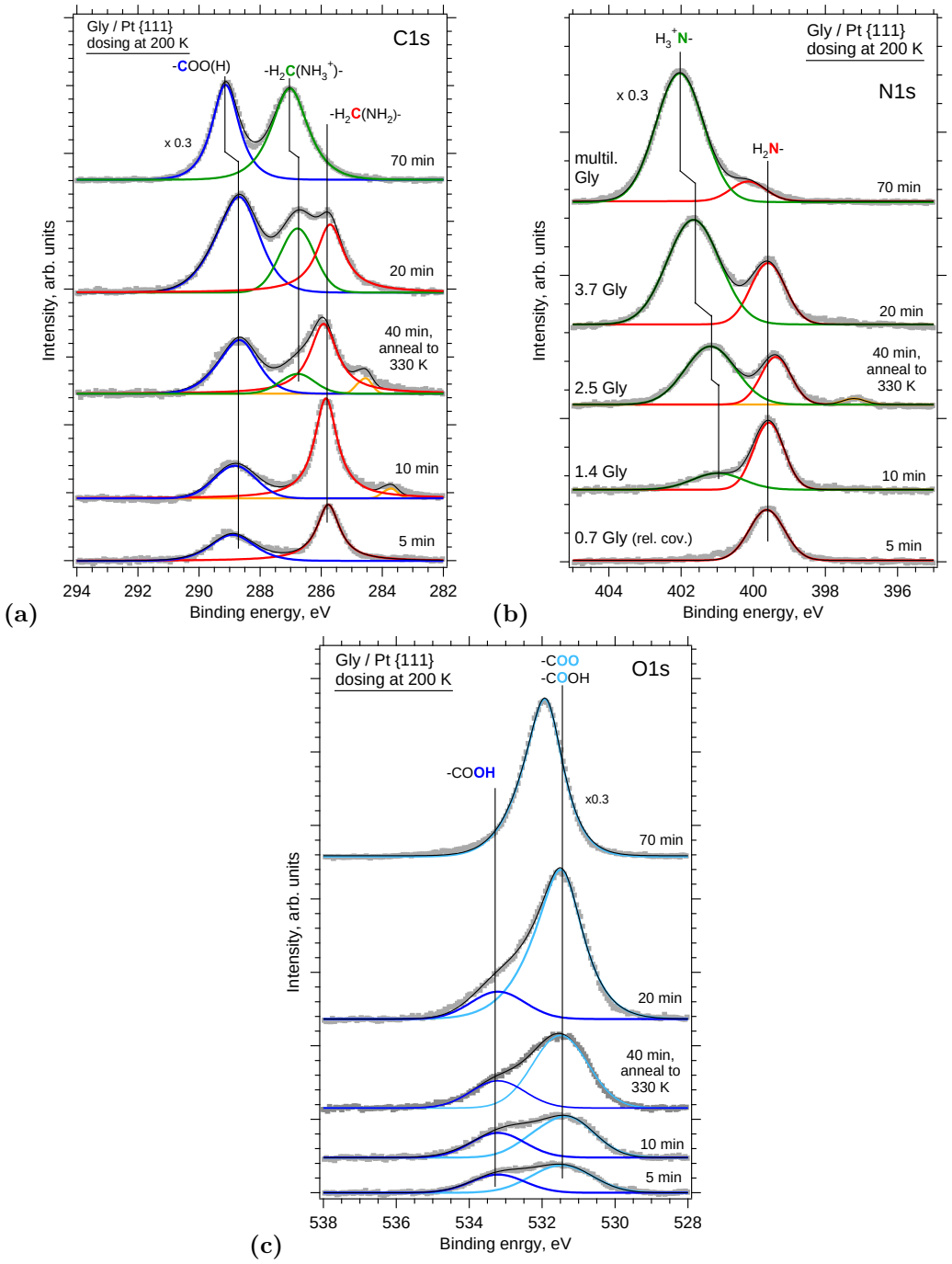

Figure 1: C 1s (a), N 1s (b) and O 1s (c) spectra of glycine overlayers on Pt{111} prepared by dosing at a sample temperature of 200 K for the indicated times, except for the middle spectra, which were recorded after annealing a multilayer (40 min dose) to 330 K. The relative coverages indicated at the left-hand side of (b) are with respect to the saturated area of the peak at BE 399.6 eV; see text for details. (Photon energies 400 eV, 525 eV and 650 eV for C 1s, N 1s and O 1s regions)

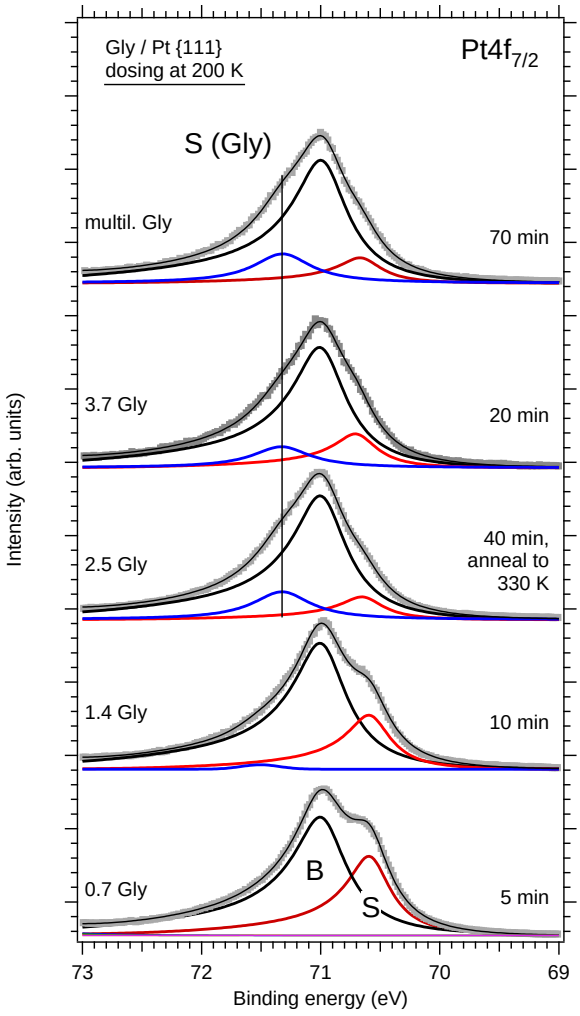

Figure 2: Pt $4f_{7/2}$ spectra for glycine overlayers on Pt{111} prepared by dosing at a sample temperature of 200 K for the indicated times. The relative coverages indicated at the left-hand side are with respect to the saturated area of the peak at BE 399.6 eV; see text for details. The spectra are normalized such that the integrated peak area is the same for all spectra. (Photon energy 205 eV).

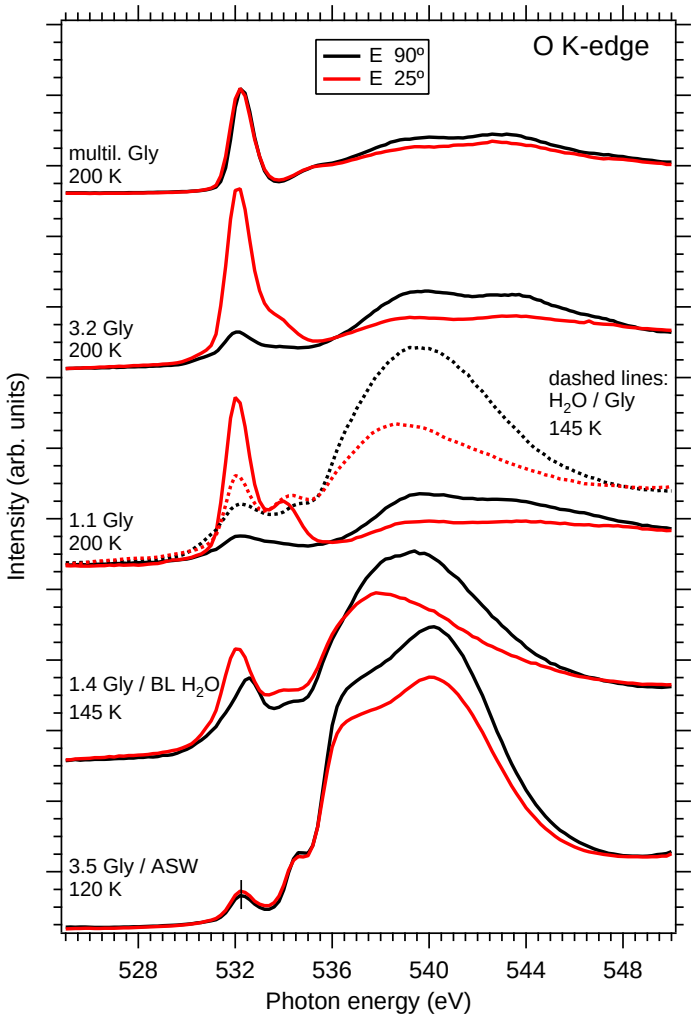

Figure 3: O K-edge NEXAFS spectra of glycine overlayers with (top down) multilayer coverage at 200K, rel coverage 3.2 Gly at 200 K (strongly bound zwitterionic) , 1.1 Gly at 200 K (neutral species), 1.1 Gly coadsorbed with 0.7 ML water (H_2O / Gly, dashed lines), 1.4 Gly adsorbed on 0.7 ML water at 145 K, and 3.5 Gly adsorbed on a thick layer of amorphous solid water (ASW) at 120 K. Spectra were taken at normal (dark, $\vec{E}$ 90° from surface normal) and grazing incidence (light/red, $\vec{E}$ 25° from surface normal).

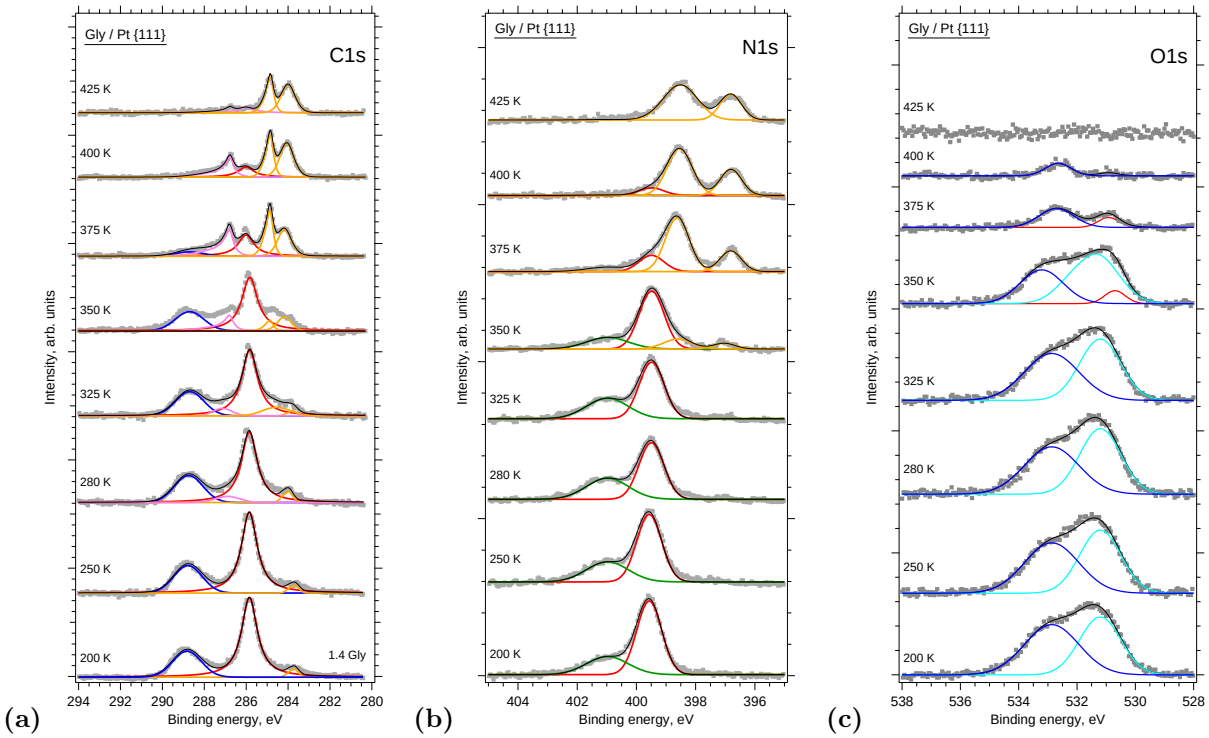

Figure 4: C 1s (a), N 1s (b), and O 1s (c) spectra of glycine (rel. coverage 1.4 Gly) adsorbed on Pt{111} at 200 K and step-annealed to the indicated temperatures. The data were recorded at 200 K. (Photon energies 400 eV, 525 eV and 650 eV for C 1s, N 1s and O 1s, respectively)

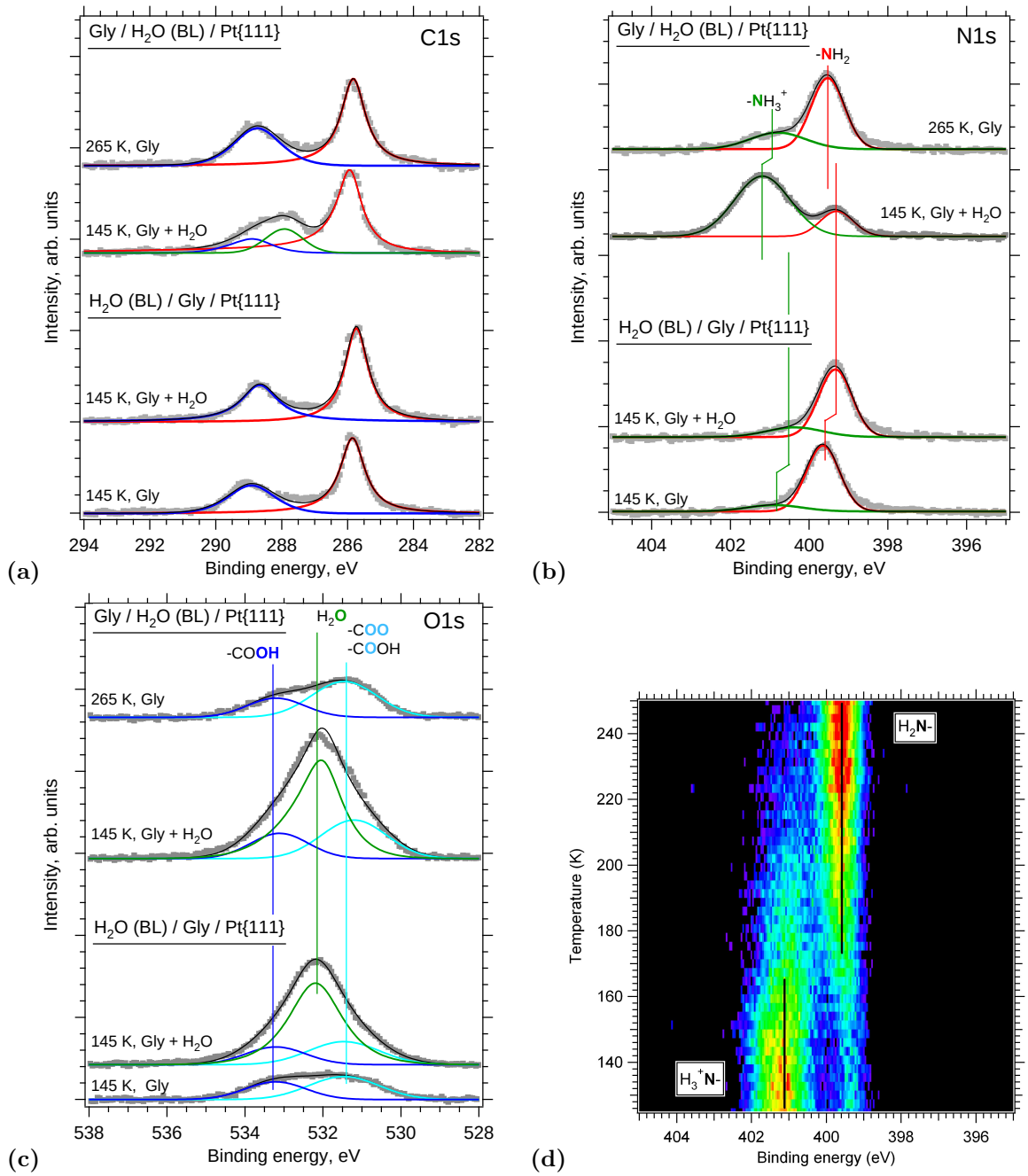

Figure 5: C 1s (a), N 1s (b) and O 1s (c) spectra of glycine overlayers on Pt{111} co-adsorbed with water with different dosing sequences. Top spectra: glycine (rel. coverage 1.4) adsorbed on a chemisorbed bilayer of water (0.7 ML) at 145 K; the '265 K' spectra were recorded after desorption of water from the surface. Bottom spectra: glycine (rel. coverage 1.2) adsorbed at 200 K, spectrum recorded at 145 K and 0.7 ML water adsorbed on the same glycine layer at 145 K. (d) TP-XPS plot (intensity vs binding energy and sample temperature) of glycine (rel. coverage 1.2) adsorbed on H_2O/Pt{111} between 160 K and 250 K. (Photon energies 400 eV, 525 eV and 650 eV for C 1s, N 1s and O 1s, respectively)

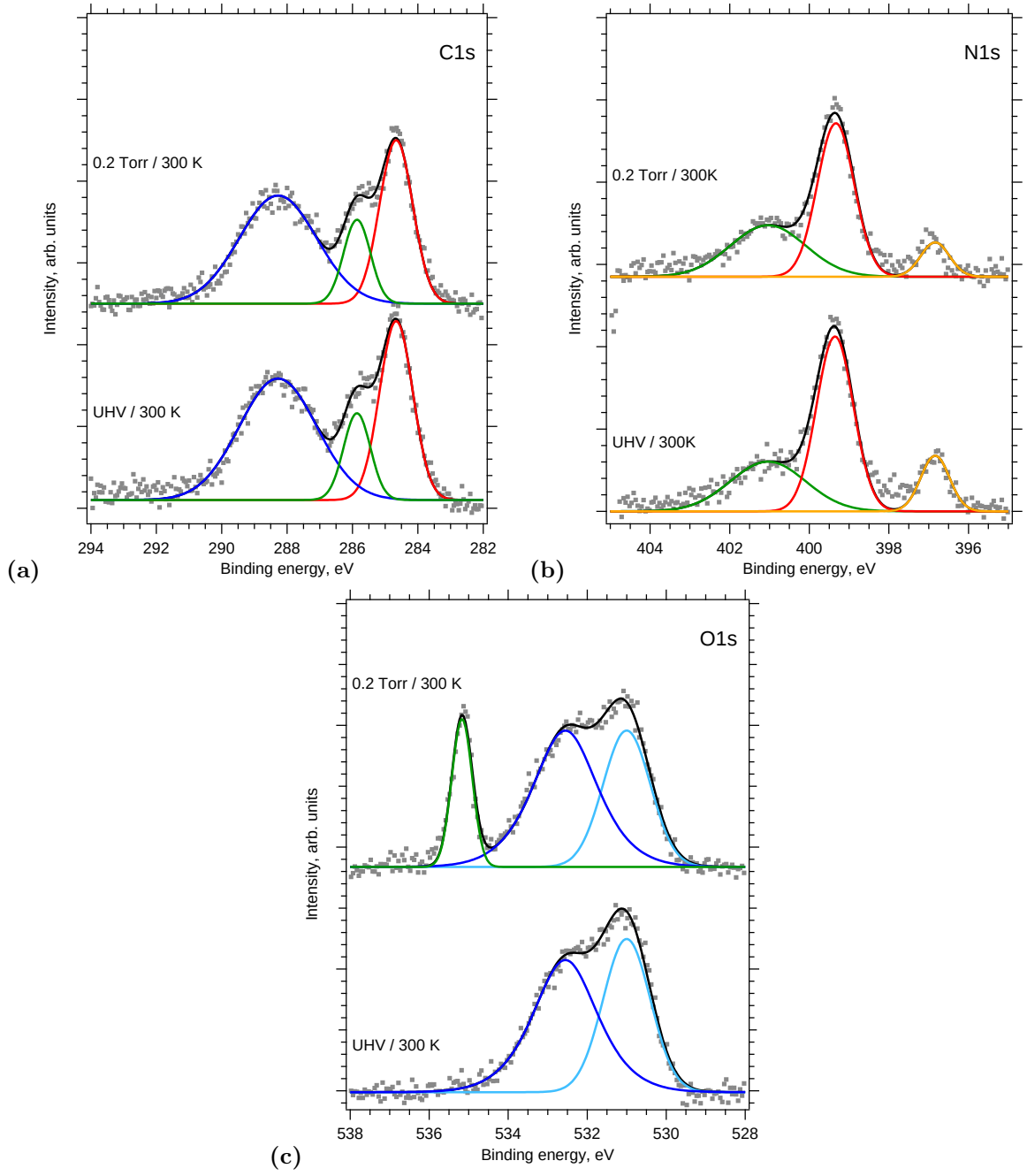

Figure 6: C 1s (a), N 1s (b) and O 1s (c) spectra of glycine overlayers on Pt{111} (rel. coverage 1.5) at 300 K in UHV (bottom spectra) and in ambient water pressure of 0.2 Torr (top spectra). (Photon energies 400 eV, 525 eV and 650 eV for C 1s, N 1s and O 1s, respectively)

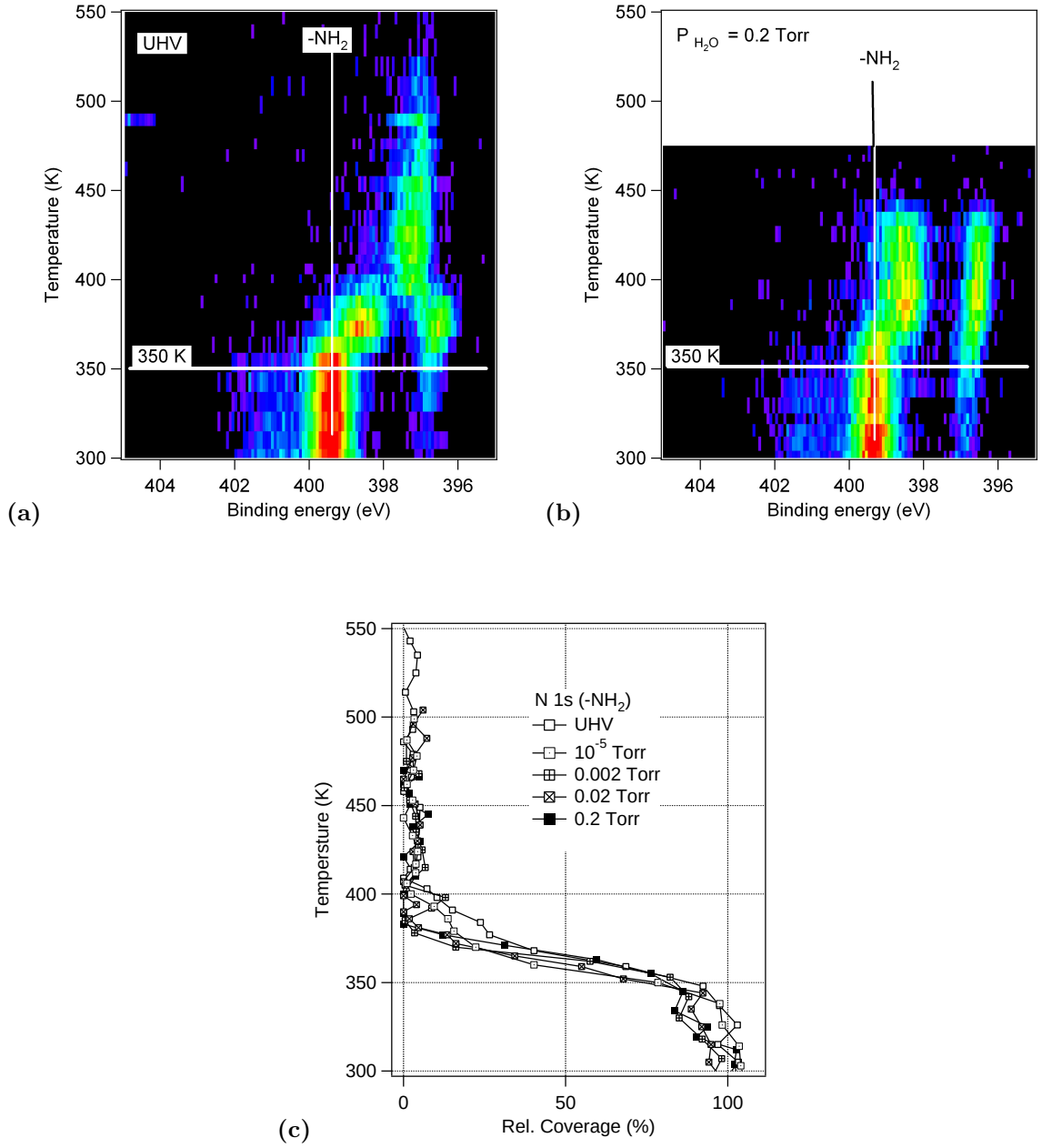

Figure 7: (a),(b) N 1s TP-XPS plots (intensity vs binding energy and sample temperature) of glycine (rel. coverage 1.5) adsorbed on Pt{111} in UHV (a) and in ambient water pressure of 0.2 Torr (b) (Photon energy 525 eV). (c) Area of the N 1s peak at 399.6 eV vs temperature. See text for details.